Appl. Phys. A 86, 441–446 (2007)
DOI: 10.1007/s00339-006-3793-8

Applied Physics A
Materials Science & Processing

Invited paper

E. JUÁREZ-RUIZ[1]
U. PAL[2]
J.A. LOMBARDERO-CHARTUNI[3]
A. MEDINA[4]
J.A. ASCENCIO[5,✉]

Chemical synthesis and structural characterization of small AuZn nanoparticles

[1] Facultad de Ciencias de la Electrónica, Universidad Autónoma de Puebla, 18 Sur y San Claudio, C.U., Puebla, Puebla 72570, Mexico
[2] Instituto de Física, Universidad Autónoma de Puebla, PO Box J-48, Puebla 72570, Mexico
[3] Universidad La Salle Benavente, 25 Ote. 9, Col. El Carmen, Puebla 72000, Mexico
[4] Universidad Michoacana de San Nicolas de Hidalgo, "Edif. U", C. U., Morelia 58000, Mexico
[5] Ductos, Corrosion y Materiales, Instituto Mexicano del Petróleo, Lazaro Cardenas 152, Col San Bartolo Atepehuacan México, Distrito Federal 07730, Mexico

Received: 27 October 2006/Accepted: 31 October 2006
Published online: 16 January 2007 •

ABSTRACT In this paper, we report the aqueous synthesis of bimetallic Au-Zn nanoparticles of different compositions by the simultaneous reduction technique. The stability and atomic configuration of the particles are studied through high-resolution transmission electron microscopy (HRTEM) and UV-Vis optical absorption techniques. Depending on the composition, small bimetallic nanoparticles of 1–15 nm in size were obtained. The average size and size distribution of the bimetallic nanoparticles are seen to be critically dependent on the atomic ratio of the constituting elements Au and Zn. While a 1 : 1 atomic proportion of Au and Zn produced most stable nanoparticles of smallest average size, nanoparticles produced with higher content of either of the component elements are unstable, inducing agglomeration and coalescence to form elongated structures with uneven morphologies. Au_3Zn_1 nanoparticles followed a directional growth pattern, producing bimetallic nanorods with multiple crystalline domains. Interestingly, in these rod-like nanostructures, the domains are in well array of solid solution-like bimetallic and pure mono-metallic regions alternatively. Such nanostructures with uneven morphology and compositions might show distinct catalytic selectivity in chemical reactions.

PACS 61.46.-w; 87.64.Ee; 74.62.Bf

1 Introduction

Application of nanotechnology in several fields is driven by the use of a variety of nanostructures. Even only the small metallic clusters have a wide range of applications, from catalysis, optics, sensors to medicine because of their singular properties derived from their nanometric size [1–5], where the quantum size effects are prominent and a high amount of atoms are exposed on the surface. One of the most important parameters that make the small particles unique is their chemical selectivity, governed from their structure, size, and elemental composition [6, 7]. Therefore the synthesis of metallic nanoparticles of desired size, shape, and composition is of great technological interest.

✉ Fax: +52 55 91756429, E-mail: ascencio@imp.mx

Bimetallic nanoclusters, in particular, have demonstrated to be most attractive for catalytic applications [3–6] with several important advantages over the monometallic ones. The interaction between two different types of atoms induces new physical properties [8–10]. In particular, Au atoms have already been tested with excellent catalytic properties when they are combined with Pt [3, 11], Pd [6, 8], Ag [12], Cu [13] and several other elements [14–16]. In our case, we used the chemical synthesis process to induce the aggregation of Au and Zn atoms, which is particularly interesting before due to the difference in aggregation tendencies of Au and Zn atoms complicating the situation in nanometer scale, where just a few atoms must aggregate. Even when Yasuda and Mori declared an spontaneous alloy of these elements, and they used electron diffraction patterns to support the formation of Au_3Zn_1 and AuZn clusters, the average measurements did not allow the determining of the real structure of the produced nanoparticles [17]. Also they could not explain a reproducible method to generate this kind of alloy, which must be because of the mentioned parameters that involve these elements and have been also studied theoretical by Tanaka et al. [18]. However, in order to improve our knowledge of the cluster formation mechanisms and the production of totally new chemical selective arrays, these bimetallic clusters are prepared. Also, these bimetallic structures could open a wide scope of applications because of the inherent properties of the elements and the generation of alternative shapes.

As the unique properties of these small clusters are governed from their structure, size and elemental composition, optical and structural characterizations of these clusters using UV-Vis spectroscopy and transmission electron microscopy (TEM) along with composition analysis are very important in understanding their growth behavior and controlling parameters before applying in technology.

We report the synthesis of AuZn nanoparticles of desired compositions and study of their stability through temporal evolution analysis. Bimetallic nanoparticles with elemental proportions of Au_1Zn_1, Au_1Zn_3 and Au_3Zn_1 are synthesized by a simultaneous chemical reduction. UV-Vis spectroscopy and high-resolution TEM (HRTEM) imaging are used to monitor the temporal evolution of the particles, structure, along with their surface passivation conditions. Depending on

the composition, bimetallic nanoparticles and nanorod structures with different surface morphologies are detected in the samples, which as far as we know, are not reported earlier.

2 Experimental methods

2.1 *Nanoparticle synthesis*

Bimetallic nanoparticles of Au-Zn are prepared by a simultaneous reduction of the chloride metal salts in water. Ionic solution of gold of 6.0×10^{-4} molar was prepared by dissolving corresponding amount of $HAuCl_4 \cdot 3H_2O$ in 70 ml of water. Similarly, the zinc ion solution of 6.0×10^{-4} molar was prepared by dissolving $ZnCl_2 \cdot H_2O$ in 70 ml of water. For the preparation of bimetallic particles, 10 ml of metal ion solution with desired proportion of Au and Zn ions was mixed with 30 mg of PVP (polyvinylpyrrolidone, $M_w = 10\,000$) (PVP) under magnetic agitation. Then approximately 0.5 ml of freshly prepared aqueous solution of $NaBH_4$ (0.025 M) was added to it at room temperature. An immediate change in color of the gold and bimetallic ion solutions indicated the formation of corresponding nanoclusters. For time evolution studies, UV-Vis optical absorption spectra of the colloidal samples preserved in dark and at room temperature were acquired at different intervals of time.

2.2 *Characterization techniques*

Structural characterization of the samples was made using a Tecnai 20 TEM with field-emission gun by FEI, with spherical aberration of 1 mm, minimal information limit of 0.15 nm and direct dot-to-dot maximum resolution of 0.23 nm, for high-resolution images, respectively. For microscopic observations, the samples were prepared by spreading a droplet of colloidal solution of Au-Zn nanoparticles onto a carbon film supported by a Cu grid and subsequent drying in vacuum. The samples were analyzed by high-resolution microscopy and the elemental composition was mapped by high-angle annular dark field imaging and the energy dispersive spectroscopy (EDS). HRTEM images were digitally processed by using filters in the Fourier space. A Shimadzu UV-3101PC double-beam spectrophotometer with slit wavelength of 2 nm and light-path length of 1 cm was used to record the absorption spectra in the wavelength range 250–800 nm of the colloids.

3 Results and discussion

The colloidal nanoparticles produced by simultaneous reduction method were studied by optical absorption spectroscopy and electron microscopy techniques in order to understand the effects of the chemical composition (the ratio of Au and Zn atoms) of the nanoparticles on the formation, size, shape, and temporal evolution after synthesis. The temporal evolution of the particles is seen to be related to their surface passivation, particularly for the synthesis method used in this work. The use of UV-Vis absorption spectroscopy allows studying the temporal evolution of the colloidal particles through monitoring their surface plasmon resonance (SPR) peaks at different intervals of time after synthesis. In Fig. 1, we can see the temporal evolution of the SPR bands for the samples Au_1Zn_1 (Fig. 1a) and Au_3Zn_1 (Fig. 1b). The drastic change in SPR peak intensity along with a gradual change

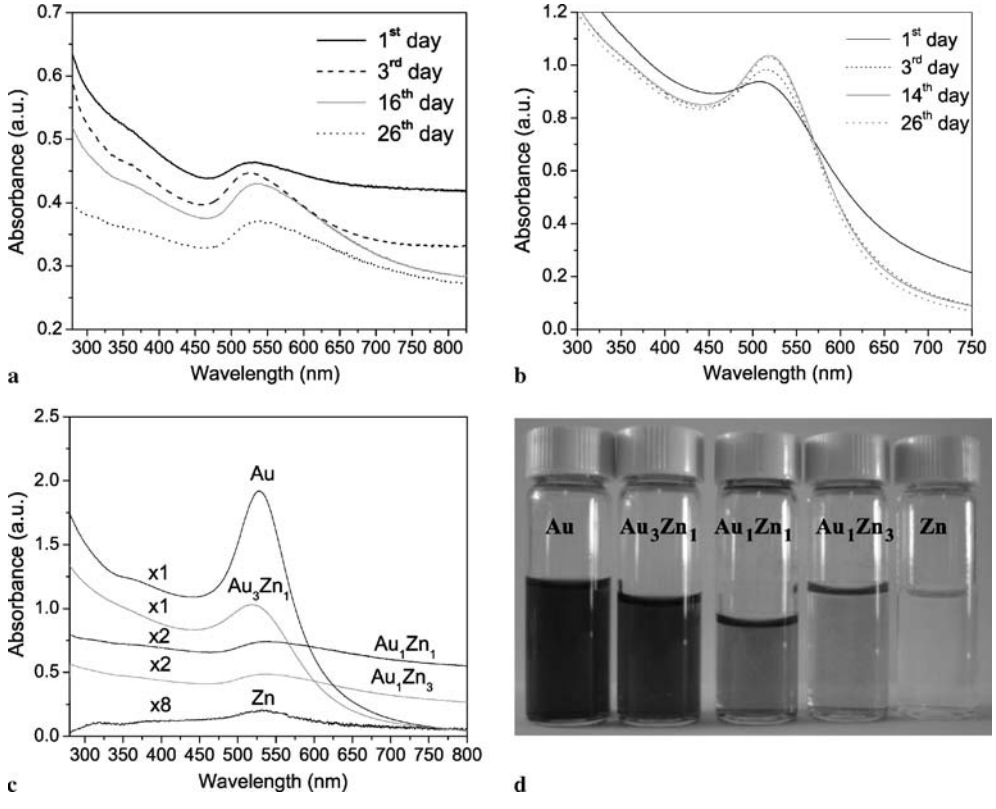

FIGURE 1 Optical analysis of Au-Zn samples. UV-Vis spectra for Au_1Zn_1 (**a**) and Au_3Zn_1 (**b**) at different intervals; absorption spectra of the samples on 26th day after preparation (**c**), and photograph of the stable colloidal solutions with different compositions showed by darker solutions (**d**)

in peak positions occur during the first 2 weeks, indicating gradual growth of the nanoparticles. After this, the particles stabilize with not much change in their SPR peak positions or intensity. While for a high concentration of Zn, the intensity of SPR band decreased with time along with a red shift in position. For high concentration of Au, the peak intensity increased without any shift in position. Such behaviors indicate a slow incorporation rate of Zn atoms in the nanoparticles. On incorporation of Zn, the SPR band of the colloidal particles becomes broader and shifts slightly towards lower energy. A clear picture of all the above characteristics is presented in Fig. 1c and d, where the optical absorption spectra of the samples with different compositions and their corresponding colors are presented, respectively.

The optical behavior of the samples is directly associated with the formation of nanoparticles and their size evolution. Therefore, a microscopic study is indispensable to evaluate the size and structure of the nanoparticles in order to understand the aggregation process and the mechanisms involved.

Figure 2 shows the typical TEM micrographs (Fig. 2a) of Au, Au_1Zn_1, Au_1Zn_3, and Au_3Zn_1 along with a typical EDS spectrum of the sample Au_1Zn_1. Apart from the signals from the microscopic copper grid (sample holder), we could not detect any other signal except the constituents Au and Zn, which indicates that the nanoparticles are of high purity. Size-distribution curves of the nanoparticles were drawn after analyzing more than 200 particles for each sample, and is shown in Fig. 2c.

	Au	Au_1Zn_1	Au_1Zn_3	Au_3Zn_1
Arithmetic media	2.35	2.67	4.74	5.86
Standard deviation	5.77	1.62	2.67	3.46

TABLE 1 Statistical analysis of synthesized nanoparticles

From the size-distribution plots and with help of Table 1, we can identify that more than 67% of the Au particles are distributed in a size range less than 4 nm, with an arithmetic media of 2.35 nm and a statistical standard deviation (SD) of 5.77 nm. Only about 12% of Au nanoparticles are bigger than 8 nm. For the sample Au_1Zn_1, the size-distribution plot reveals a similar behavior, with an AM = 2.67 nm and a SD = 1.62, indicating a better homogeneity in size than its monometallic counterpart Au. Furthermore, the

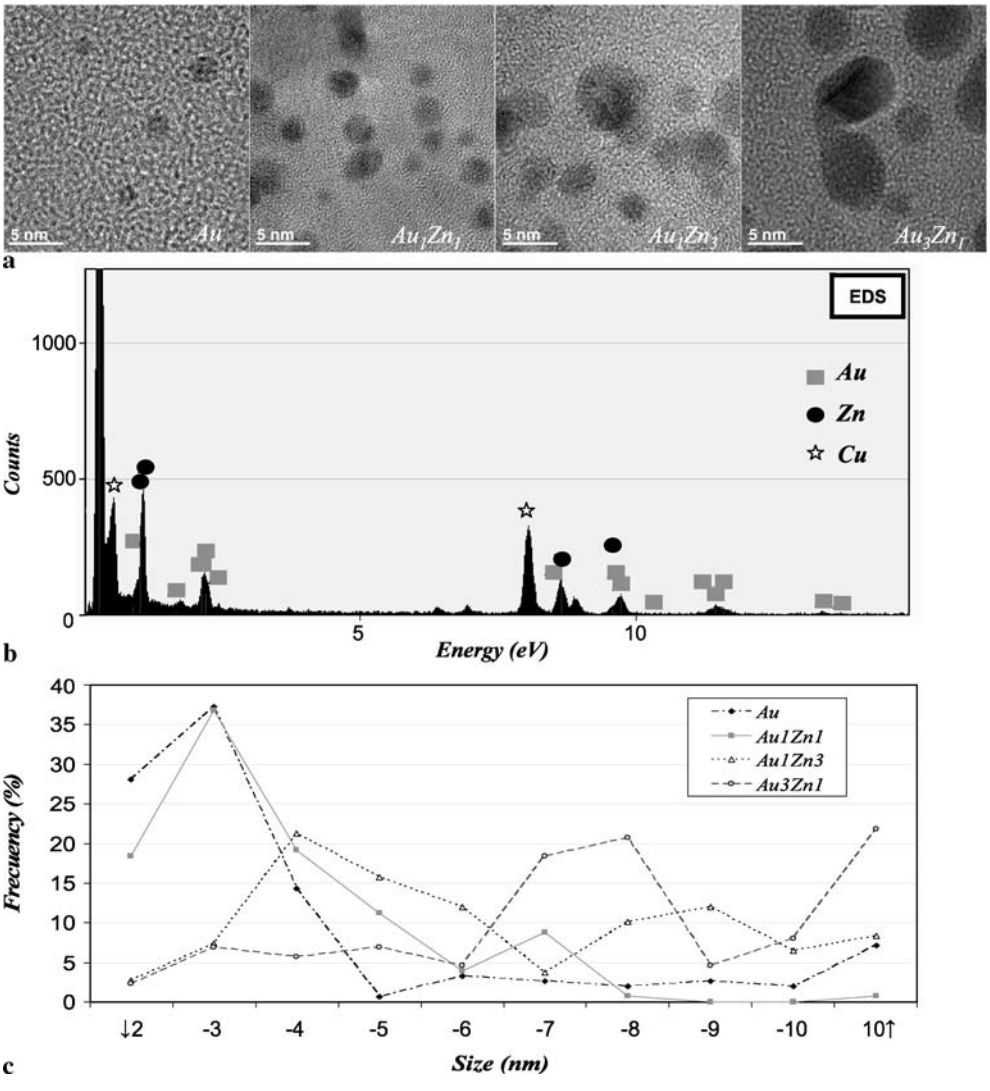

FIGURE 2 TEM and composition analysis of the synthesized samples: typical TEM micrographs of the colloidal clusters of different compositions (**a**), EDS spectrum for Au_1Zn_1 sample (**b**) and size distribution plots for the samples with different compositions (**c**)

size-distribution plot of Au_1Zn_3 sample revealed AM = 4.74 and SD = 2.67 nm, while for Au_3Zn_1, AM = 5.86 nm and SD of 3.46 nm. These results denote that the size dispersion is least for the sample Au_1Zn_1. The dispersion increases when the concentration of either of the components is high. The effect is more prominent for Au than Zn as it has been probed by different elements with stronger atomistic interactions.

To understand the mechanism of formation of the bimetallic nanoparticles and their anomalous size distributions we use HRTEM to study their morphology, internal crystalline structure, and hence their stability.

In Fig. 3, the HRTEM analysis for the pure Au nanoparticles is presented. We can find a multiple twined nanoparticle of 3.8 nm in Fig. 3a, and an fcc-like particle of about 3.6 nm in Fig. 3b, with characteristic FTTs. An interesting structure is identified in Fig. 3c, which can be associated with a single twin particle of about 2.4 nm, with characteristic dots splitting in its FFT. Images in Fig. 3d and e demonstrate the evidence of formation of bigger structures, which must have been produced due to coalescence of several small particles. The corresponding FFT patterns also demonstrate that they correspond to polycrystalline structures with linear array along some preferential direction (Fig. 3d), or grow along multiple directions with arbitrary orientations (Fig. 3e, with multiple reflections in FFT spectrum). In the last structure, in particular, the inter-planer distance varied drastically from grain to grain.

Nanoparticles in the sample Au_1Zn_1 revealed structures similar to pure Au though their size distribution is different. From the typical HRTEM images of the particles presented in Fig. 4, we can observe an fcc-like particle of 2.4 nm (Fig. 4a), a single twin particle of about 4.3 nm (Fig. 4b), a couple of multiple twined particles of about 3.4 and 4.6 nm with decahedron (Fig. 4c) and icosahedron (Fig. 4d) geometries, respec-

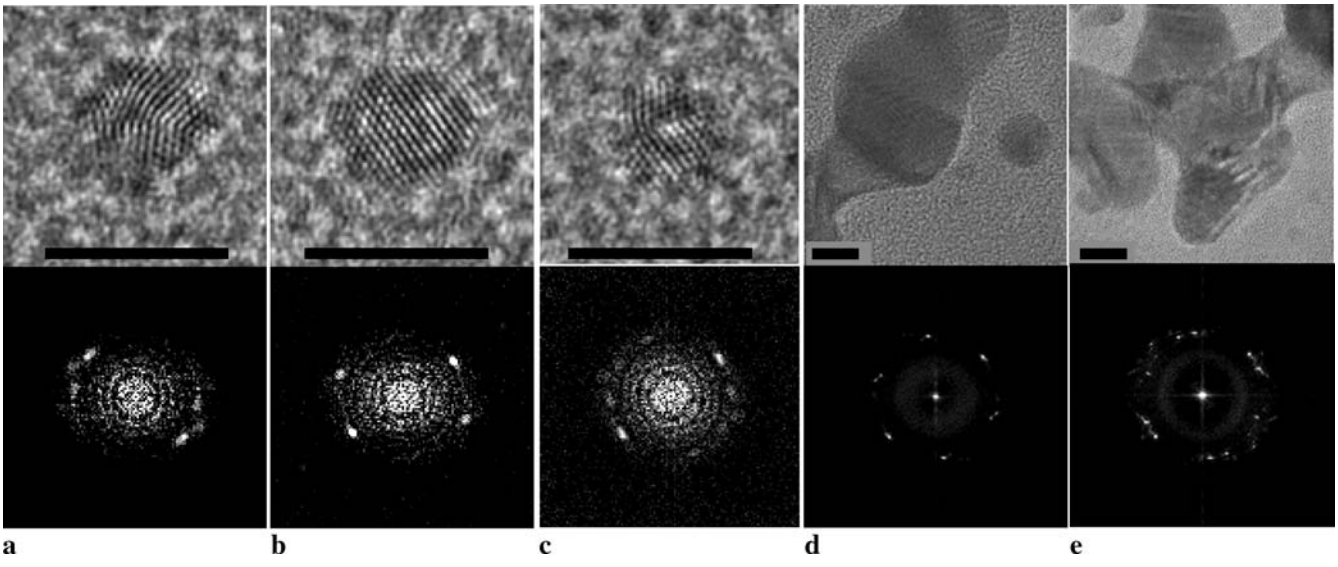

FIGURE 3 HRTEM analysis of pure Au sample: multiple twin (**a**), fcc-like (**b**) and single twin nanoparticles (**c**); besides structure where coalescence of smaller particles are evident in linear (**d**) and arbitrary shaped (**e**). FFT patterns are shown for each image (*scale bar* 5 nm)

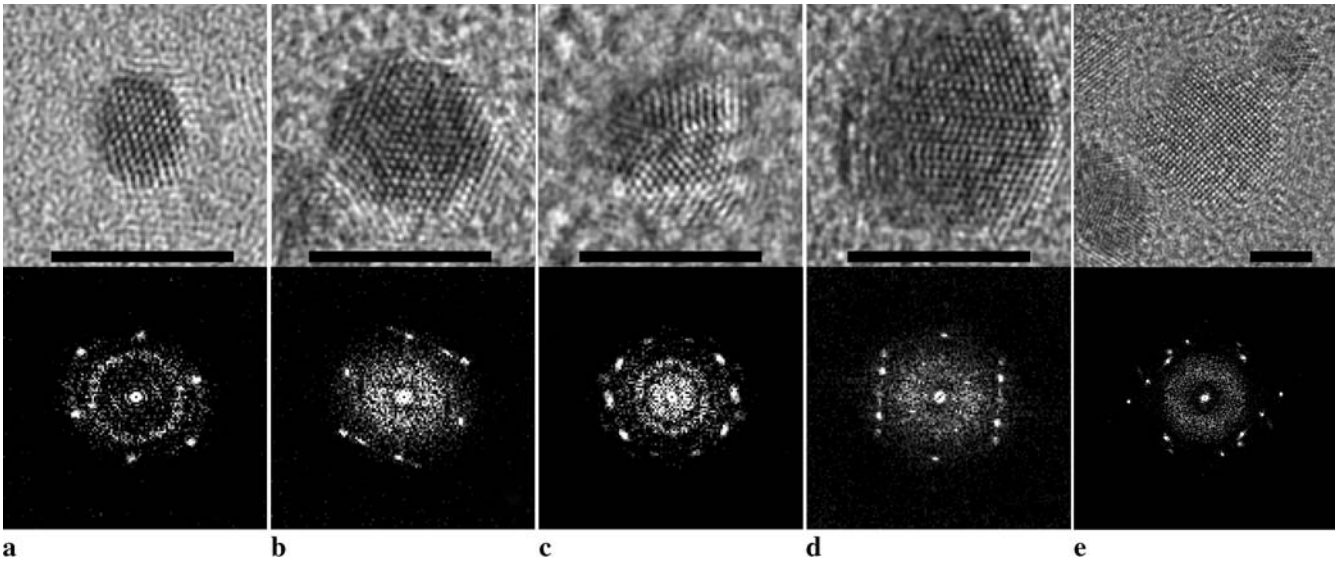

FIGURE 4 Typical HRTEM images of Au_1Zn_1 nanoparticles: fcc-like (**a**), single twin (**b**), decahedral (**c**) and icosahedral nanoparticles (**d**); besides a bigger structure with cubic array (**e**). FFT patterns are shown for each image ((*scale bar* 5 nm)

tively. While the decahedron is in five-fold view, the icosahedron is observed in a lateral view [19]. Clusters bigger than 10 nm, rarely observed in this sample, revealed atomistic contrast due to a big defocus, which has been identified for focal series of mono metallic and bimetallic nanoparticles [20, 21]. Distinct inter-planer spacing values determined from their FFTs is due to the presence of neighboring particles, indicating the co-existence of different atomistic structures in the sample.

The most common types of contrasts revealed from the HRTEM images of the sample Au_1Zn_3 are shown in Fig. 5. We can observe an fcc-like nanoparticle of about 4.4 nm in size with evidence of rhombic and hexagonal combined contrasts in Fig. 5a. While a single twin particle of about 5.2 nm is shown in Fig. 5b, a multiple twined particle of about 9.8 nm size with a shape derived from hexagonal structure can be seen in Fig. 5c. Bigger clusters produced by coalescence of two or more smaller particles are also identified in the sample. In Fig. 5d, we can observe an oval-shaped particle of about 13 nm in size produced through coalescence of two similar size particles. A 5-nm particle attached to another particle of about 14 nm in size forming a bigger structure can be observed in Fig. 5e. Production of bigger clusters associated with the aggregation and following coalescence processes indicates the presence of large quantity of un-passivated structures in the sample generating bi-modal size distribution in their size-distribution curves (Fig. 1c).

Finally, when the amount of Zn is minor, i.e., in the case of Au_3Zn_1 nanoparticles, the characteristics of the particles are quite different. No single-crystalline particle could be found

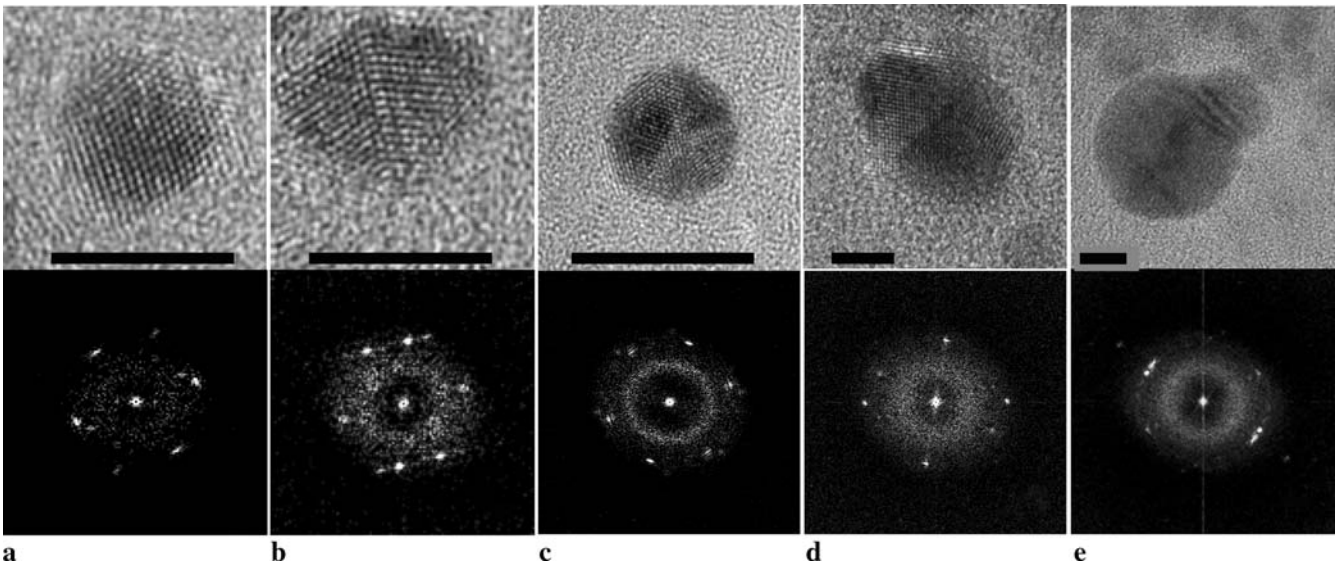

FIGURE 5 HRTEM analysis of Au_1Zn_3 nanoparticles: fcc-like (**a**), single twin (**b**) and multiple twin (**c**) (at five-fold orientation) nanoparticles; coalescence of particles are observed for a couple of similar size particles (**d**) and two of them with different dimensions (**e**). FFT patterns are shown for each image (*scale bar* 5 nm)

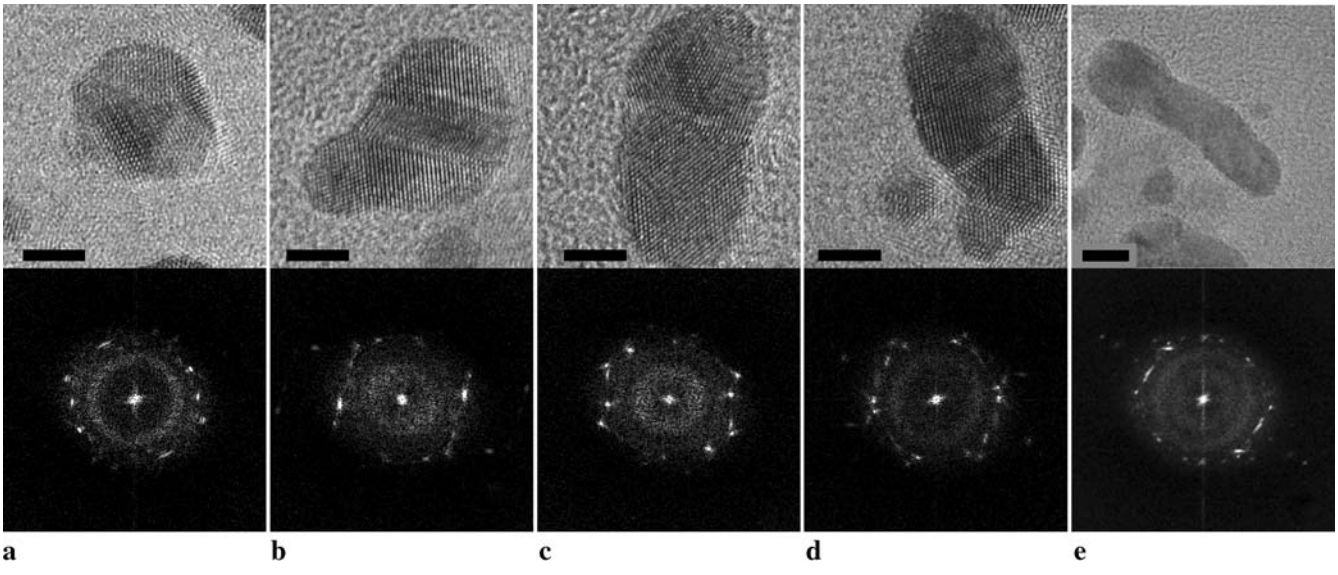

FIGURE 6 HRTEM analysis of Au_3Zn_1 nanoparticles: three domains cluster (**a**), multiple steps structure under coalescence (**b**), irregular rod (**c**) and particle aggregating to bigger structure (**d**) and irregular surface nanorod (**e**). FFT patterns are shown for each image (*scale bar* 5 nm)

in this sample. Most of the particles are big and are apparently produced by aggregation of smaller particles. While in Fig. 6a, we can observe a distorted particle of about 11 nm in size with multiple inter-planer spacings (as can be seen from FFT), a 5-nm particle attached to a bigger particle with several atomistic step-contrasts can be seen in Fig. 6b. Such aggregation characteristics are commonly observed during the formation of metallic nanorods, where aggregation of particles following a growth axis determines the shape of the one dimensional nanostructures [22–24]. We could identify a huge number of such structures in this sample. As example, we can observe an elongated structure with three distinct domains in Fig. 6c, with an aspect ratio of 3 (8×23 nm). Such aggregation process is even clearer in the micrograph of Fig. 6d captured while a particle of 3.8 nm is being attached to a rod of 7 nm wide and 22 nm length containing four domains. A more generalized picture of the aggregation process can be obtained from the Fig. 6e, where a multi-domain, rod-like structure of aspect ratio 6 with irregular surface can be observed. The multiple crystalline sections that produce the structures can be distinguished from the corresponding FFT spectra by measuring the inter-planer distances. Inter-planer distances of 3.14 Å and 2.23 Å measured in some regions (marked as A) correspond to the structures of Au-Zn alloy [25]; while there are other sections with distances of 2.35 Å and 2.05 Å (marked as B) that match with pure Au.

Structural peculiarities of these nanoparticles must have been driven by the concentration of their constituting components. As described earlier, produced pure Au nanoparticles are very small in size with a tendency to aggregate into much bigger clusters. On the other hand, for the sample Au_1Zn_1, the aggregates show a homogeneous size distribution with highly stabilized shapes. The difference in elemental concentration in the bimetallic samples not only induces the growth of bigger clusters through their coalescence, but also induces their irregular forms, as in the case of Au_1Zn_3. In the case of Au_3Zn_1, the coalescence of nanoparticles induces the generation of one-dimensional shapes as nanorods, with well-identified multiple domains and irregular surfaces. Interestingly, in these rod-like nanostructures, the domains are in well array of solid solution-like bimetallic and pure mono-metallic regions alternatively. Such irregular morphologies and domain structures with inhomogeneous compositions are driven by the relative concentration of component ions.

4 Conclusions

In summary, we could prepare bimetallic Au-Zn nanoparticles with varying compositions by simultaneous chemical reduction technique. The size of the nanoparticles depends strongly on their composition. While a 1 : 1 proportion of the Au and Zn (i.e. Au_1Zn_1) produces smallest and stable clusters, unequal proportions of Au and Zn (e.g. Au_1Zn_3 and Au_3Zn_1) generate unstable clusters that frequently coalesce to form bigger structures. Of particular interest is the case of Au_3Zn_1, where the aggregation of particles follows directional growth producing bimetallic nanorods. While these one-dimensional nanostructures with uneven morphology and compositions might show distinct catalytic selectivity in chemical reactions, their domain array of alternating compositions opens up a great interest to study their mechanical behaviors.

REFERENCES

1 H.S. Nalwa, *Handbook of Nanostructured Materials and Nanotechnology* (Academic Press, San Diego, 2000)
2 J.A. Ascencio, A.C. Rincon, G. Canizal, J. Phys. Chem. B **109**, 8806 (2005)
3 R. Esparza, J.A. Ascencio, G. Rosas, J.F. Sanchez-Ramirez, U. Pal, R. Perez, J. Nanosci. Nanotechnol. **5**, 641 (2005)
4 R. Narayanan, M.A. El-Sayed, J. Phys. Chem. B **109**, 12 663 (2005)
5 A. Morlang, U. Neuhausen, K.V. Klementiev, F.W. Schutze, G. Miehe, H. Fuess, E.S. Lox, Appl. Catal. B **60**, 191 (2005)
6 M.O. Nutt, J.B. Hughes, M.S. Wong, Environ. Sci. Technol. **39**, 1346 (2005)
7 C.N.R. Rao, A. Müller, A.K. Cheetham, *Chemistry of Nanomaterials: Synthesis, Properties and Applications* (Wiley, New York, 2004)
8 H.B. Liu, U. Pal, A. Medina, C. Maldonado, J.A. Ascencio, Phys. Rev. B **71**, 075 403 (2004)
9 H.C. Chu, S.R. Sheen, C.T. Yeh, T.P. Perng, J. Alloys Compd. **322**, 198 (2001)
10 F. Dassenoy, M.J. Casanove, P. Lecante, C. Pan, K. Philippot, C. Amiens, B. Chaudret, Phys. Rev. B **63**, 235 407 (2001)
11 J.L. Rodriguez-Lopez, J.M. Montejano-Carrizales, U. Pal, J.F. Sanchez-Ramirez, H.E. Troiani, D. Garcia, M. Miki-Yoshida, M. Jose-Yacaman, Phys. Rev. Lett. **92**, 196 102 (2004)
12 R. Mitric, C. Bürgel, J. Burda, V. Bonacic-Koutecký, P. Fantucci, Eur. Phys. J. D **24**, 41 (2003)
13 J.A. Ascencio, H.B. Liu, U. Pal, A. Medina, Z.L. Wang, Microsc. Res. Technol. **69**, 522 (2006)
14 D.I. Garcia-Gutierrez, C.E. Gutierrez-Wing, L. Giovanetti, J.M. Ramallo-Lopez, F.G. Requejo, M. Jose-Yacaman, J. Phys. Chem. B **109**, 3813 (2005)
15 J. Yang, J.Y. Lee, H.P. Too, Anal. Chim. Acta **537**, 279 (2005)
16 J.A. Ascencio, Y. Mejia, H.B. Liu, C. Angeles, G. Canizal, Langmuir **19**, 5882 (2003)
17 H. Yasuda, H. Mori, Phys. Rev. Lett. **69**, 3747 (1992)
18 H. Tanaka, S. Neukermans, E. Janssens, R.E. Silverans, P. Lievens, J. Chem. Phys. **119**, 7115 (2003)
19 J.A. Ascencio, C. Gutierrez-Wing, M.E. Espinosa, M. Marin, S. Tehuacanero, C. Zorrilla, M. Jose-Yacaman, Surf. Sci. **396**, 349 (1998)
20 L. Cervera-Gontard, L.Y. Chang, R.E. Dunin-Borkowski, A.I. Kirkland, C.J.D. Hetherington, D. Ozkaya, J. Phys. Conf. Ser. **26**, 25 (2006)
21 D.J. Smith, J. Electron. Microsc. Technol. **12**, 11 (2005)
22 G. Canizal, J.A. Ascencio, J. Gardea-Torresday, M. Jose-Yacaman, J. Nanopart. Res. **3**, 475 (2001)
23 M.A. El-Sayed, V. Volkiv, S. Link, Chem. Phys. Lett. **317**, 517 (2000)
24 U. Pal, P. Santiago, J. Chavez, J.A. Ascencio, J. Nanosci. Nanotechnol. **5**, 609 (2005)
25 T.W. Darling, F. Chu, A. Migliori, D.J. Thoma, M. Lopez, J.C. Lashley, B.E. Lang, J.F. Boerio-Goates, B. Woodfield, Philos. Mag. B **82**, 825 (2002)